

## **Intracellular microRNAs Accurate Detection Using Functional Mo<sub>2</sub>C Quantum Dots Nanoprobe**

Wenhao Dai,<sup>a</sup> Huiting Lu,<sup>b</sup> Fan Yang,<sup>a</sup> Haifeng Dong<sup>\*a</sup> and Xueji Zhang<sup>\*ac</sup>

<sup>a</sup> *Research Center for Bioengineering and Sensing Technology, School of Chemistry and Bioengineering, University of Science & Technology Beijing, Beijing 100083, P.R. China.*

<sup>b</sup> *School of Chemistry & Biological Engineering University of Science & Technology Beijing, Beijing 100083, P.R. China*

<sup>c</sup> *School of Biomedical Engineering, Shenzhen University Health Science Center, Shenzhen, Guangdong 518060, P. R. China*

*E-mail addresses: hfdong@ustb.edu.cn (Haifeng Dong), zhangxueji@ustb.edu.cn (Xueji Zhang).*

## Experimental Section

### Materials and reagents

The molybdenum carbide ( $\text{Mo}_2\text{C}$ ) powder and 3-(4,5-dimethyl-2-thiazolyl)-2,5-diphenyl-2-H- tetrazolium bromide (MTT) were purchased from Sigma-Aldrich (China). Dimethyl sulphoxide (DMSO) was obtained from Sinopharm Chemical Reagent Co., Ltd (Beijing, China). Hoechst 33342, calcein-AM and propidium iodide (PI) were obtained from Yeasen Biotech. Co., Ltd. (Shanghai, China). Phosphate buffer saline (PBS, pH 7.4), fetal bovine serum (FBS), Dulbecco's modified Eagle's medium (DMEM), trypsin-EDTA and penicillin-streptomycin were purchased from Gibco Life Technologies (AG, Switzerland). All other chemicals used in this study were analytical reagent grade and used without further purification. The ultrapure water was obtained from a Millipore water purification system (18 M $\Omega$ , Milli-Q, Millipore, USA). All of the DNA sequences were purchased from Sangon Biological Engineering Technology & Services Co., Ltd. (Shanghai, China). The RNA sequences purified using high-performance liquid chromatography were obtained from Gene Pharma (Shanghai, China) and modified with 2'-OMe to increase resistance to nucleases to improve the stability for miRNA detection. Their sequences are as follows. All the miRNA sequences were diluted in diethyl pyrocarbonate (DEPC)-treated water for experiments, and all the experiments were performed in a laminar flow bench for a clean environment to control the influence of RNase. Before the MB were carried out experiment, they were all annealed (heat at 95 °C for 5 min, gradually cool to 25 °C at 5 °C/min, and stand at 25 °C for 1 h at least) in PBS (10 mM, pH = 7.4, with 137 mM NaCl), ensuring

the desirable hairpin structures.

### **Synthesis of Mo<sub>2</sub>C QDs**

The Mo<sub>2</sub>C QDs were synthesized as our previously reported with brief modification.<sup>1</sup> Briefly, 1 g Mo<sub>2</sub>C powder was added into 200 mL ultrapure water, and the mixture was then sonicated (400 W) for 20 h. The resulting mixture was centrifuged at 5000 rpm for 15 min to remove the flakes of Mo<sub>2</sub>C. Then, the supernatant was further purified through a 0.22 μm microporous membrane to obtain Mo<sub>2</sub>C QDs.

### **Characterization of Mo<sub>2</sub>C QDs**

The morphologies of Mo<sub>2</sub>C QDs were examined with a FEI F20 TEM (FEI, USA) and a JSM-6700FSEM (JEOL, Japan). AFM measurement was carried out on Nanoscope IIIa (Digital Instrument, USA) under tapping mode. XPS analyses were recorded with an ESCALAB 250 spectrometer (Thermo-VG Scientific, USA). Zeta potential analysis was performed on Nano ZS (Malvern, UK). An inVia-Reflex Confocal Raman spectrometer (Renishaw, UK) and XRD pattern of the as-prepared Mo<sub>2</sub>C QDs was recorded by a Bruker-AXS X-ray diffractometer with Cu Kα radiation ( $\lambda=1.5418 \text{ \AA}$ ). The UV-vis-NIR absorption was acquired with a UV-1800 spectrophotometer (Shimadzu, Japan) and processed with Origin Lab software. The size distribution and zeta potential analysis were performed using a Zetasizer Nano ZS system (Malvern, UK), and the 633 nm laser was used for the DLS. The confocal laser scanning microscopy (CLSM) images were acquired on a FV1200 microscope (Olympus). The temperature was measured by a digital thermometer with a thermocouple probe and recorded once every 2 s. An infrared thermal imaging camera

(Fluke TiS65, USA) was used to monitor the temperature change.

### **Feasibility of intracellular miRNA-21 accurate detection**

According to previous report, we have design five types of MB to test the capability to accurate detect intracellular miRNAs<sup>2,3</sup>. The mature miRNAs MB (50 nM) incubated with mature miRNA-21 (50 nM) or pre-miRNA-21 (50 nM) at 37 °C for 60 min, and detect by fluorescence spectrometer. The performance of pre-miRNAs MB was also detect in same conditions.

### **The selectivity and sensitivity of the Mo<sub>2</sub>C QDs nanoprobe**

The Mo<sub>2</sub>C QDs nanoprobe was prepared through a simple approach. Different volumes of the obtained Mo<sub>2</sub>C QDs (50 µg/mL) were mixed with miRNA-21 MB (50 nM) and pre-miRNA-21 MB (50 nM) and sonicated for 30 min to prepare Mo<sub>2</sub>C QDs nanoprobe. The MBs were adsorbed onto the surface of the Mo<sub>2</sub>C QDs through the  $\pi$ - $\pi$  interaction. Then, the Mo<sub>2</sub>C QDs nanoprobe incubated with different concentration of mature miRNA-21 and pre-miRNA-21 at 37 °C for 60 min, and detect by fluorescence spectrometer.

### **Cell culture**

The B16-F10 cells were cultured in Dulbecco's modified Eagle's medium (DMEM, GIBCO) supplemented with 10% fetal calf serum, penicillin (100 mg/mL), and streptomycin (100 mg/mL) at 37 °C in a humidified atmosphere containing 5% CO<sub>2</sub>.

### ***In vitro* cytotoxicity assay**

B16-F10 cells ( $5.0 \times 10^4$ ) were cultured for 12 h in a 96-well plate containing

DMEM (100  $\mu$ L) in each well, and then the medium was replaced with fresh serum-free medium (Opti-MEM) alone or medium containing Mo<sub>2</sub>C QDs and incubated for another 4 h. Next, MTT (20  $\mu$ L, 5 mg/mL) with fresh DMEM (100  $\mu$ L) was then added to each well. The media was removed 4 h later, and DMSO (100  $\mu$ L) was added to solubilize the formazan dye. After shocking (37 °C, 120 rpm) for 15 min, the absorbance of each well was measured using a Tecan Sunrise at 488 nm. The cytotoxicity of Mo<sub>2</sub>C QDs was estimated by the percentage of growth inhibition calculated with the formula.

$$\text{Growth inhibition \%} = (1 - A_{\text{test}}/A_{\text{control}}) 100\%$$

### **Intracellular miRNA-21 accurate detection**

B16-F10, A549, MDA-MB-231 and NHDF cells ( $1.0 \times 10^4$ ) were cultured in a confocal dish containing DMEM (1 mL) for 12 h. The media were then replaced with fresh Opti-MEM (1 mL) containing Mo<sub>2</sub>C QDs-based probe (50  $\mu$ g/mL, 50 nM loaded MB) and cultured for 4 h. After washing each dishes twice by PBS (10 mM, pH =7.4), the fresh DMEM medium (1 mL) was added and cultured for another 24 h, and detected by confocal microscope (FV1200, Olympus).

### **Quantitative detection of intracellular miRNA-21**

According to previous reports <sup>4,5</sup>, A549 cells ( $1.0 \times 10^4$ ) were cultured in a confocal dish containing DMEM (1 mL) for 12 h. 50  $\mu$ L Opti-MEM was added to different concentration of miRNA-21 mimics or 1  $\mu$ L Lipofectamine<sup>TM</sup> 2000, and the obtained two solution were mixed and diluted by 900  $\mu$ L Opti-MEM to prepare the transfected solution. The media were then replaced with prepared transfected solution and cultured

for 4 h. After washing each dishes twice by PBS (10 mM, pH =7.4), the fresh DMEM medium (1 mL) was added and cultured for another 8 h. The media were replaced with fresh Opti-MEM (1 mL) containing Mo<sub>2</sub>C QDs nanoprobe (50 µg/mL, 50 nM loaded mature miRNA MB and pre-miRNA MB) and cultured for 4 h. Eight hours later, the cells were detected by confocal microscope (FV1200, Olympus).

## Figures



**Fig. S1.** Photograph of Mo<sub>2</sub>C QDs at 20 h.

**SEM Characterization of bulk Mo<sub>2</sub>C:** The morphologies of bulk Mo<sub>2</sub>C was examined with a SU8010 scanning electron microscope (Hitachi, Japan). Fig. S2 shows the SEM images of the bulk Mo<sub>2</sub>C. The original material e Mo<sub>2</sub>C clearly reveals that the sheet is smoothly flat with a neat and delicate stepped fracture.

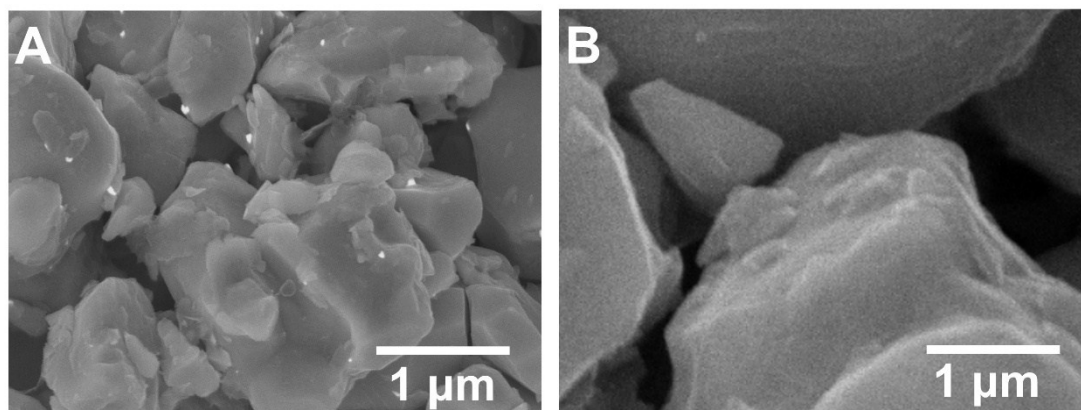


**Fig. S2.** (A) SEM image and (B) magnified image of the Mo<sub>2</sub>C powder.



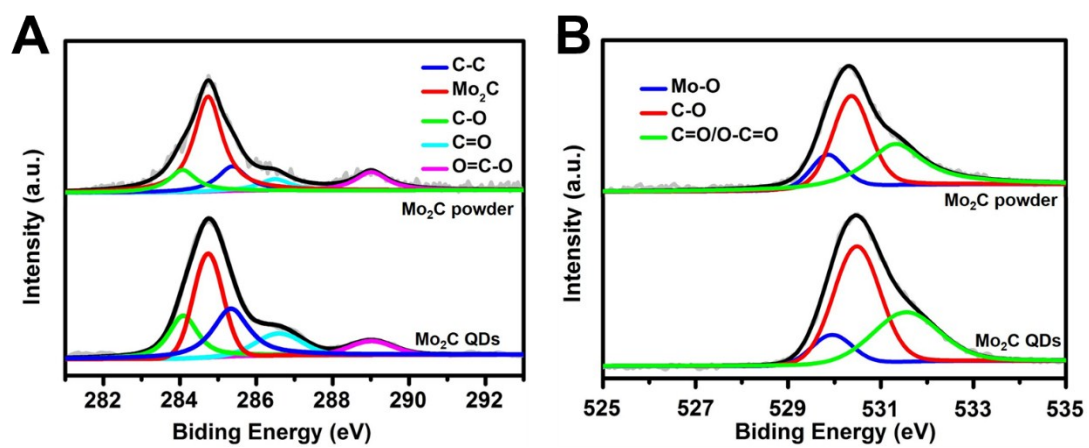


**Fig. S3.** (A) High-resolution XPS spectra showing C 1s peaks of Mo<sub>2</sub>C powder and Mo<sub>2</sub>C QDs. (B) High-resolution XPS spectra showing O 1s peaks of Mo<sub>2</sub>C powder and Mo<sub>2</sub>C QDs.

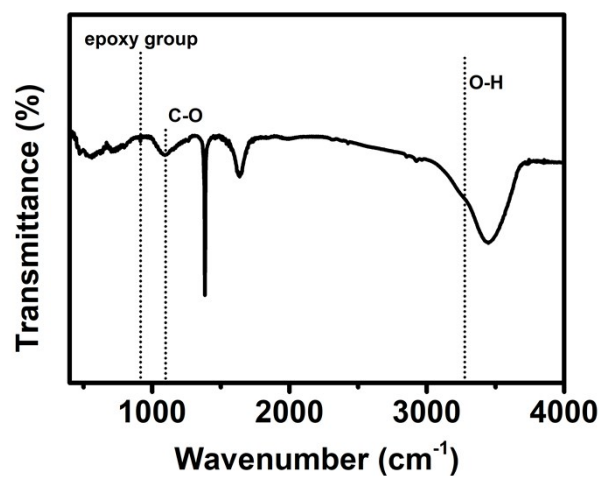


**Fig. S4.** The FTIR of the proposed Mo<sub>2</sub>C QDs nanoprobe.

**Stability and biocompatibility of Mo<sub>2</sub>C QDs:** It displayed good stability in aqueous solution including deionized water, high salt solution phosphate buffered saline (PBS) (10 mM, pH=7.4, 137 mM NaCl) and cell medium (Dulbecco's modified Eagle's medium (DMEM) supplemented with 10% fetal bovine serum (FBS), penicillin (100 mg/mL), and streptomycin (100 mg/mL)) (Fig. S5A), which was confirmed by the UV-vis-NIR absorption spectra (Fig. S6A), zeta potential analysis (Fig. S6B), and dynamic light scattering (DLS) (Fig. S6C-E). Good stability over broad pH values was also revealed (Fig. S5B). Moreover, to assess the stability of the MB loaded on Mo<sub>2</sub>C QDs, high concentration (5 U/mL) of DNase I was added to the Mo<sub>2</sub>C QDs nanoprobe for incubation with different time (0, 30, 60 min) at 37°C, and the free MB mixed with DNase I at same condition as a control (Fig. S5C). It was shown that no degradation was observed for the MB loaded on Mo<sub>2</sub>C QDs at both 30 min and 60 min incubation. However, 88.5% of the free MB was digested for 30 min, and complete hydrolyzation of the free MB was observed after 60 min incubation. It is demonstrated that the good protection capability of Mo<sub>2</sub>C QDs to prevent the MB from DNase I digestion.

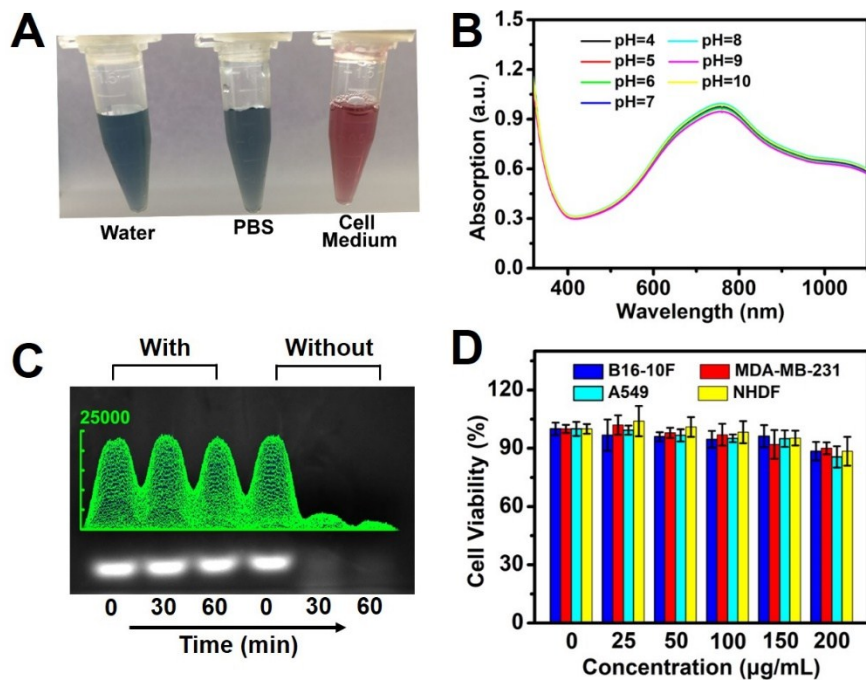


**Fig. S5.** (A) Photograph of the Mo<sub>2</sub>C QDs in different conditions taken under visible light. (B) pH-dependent UV-vis-NIR spectra of Mo<sub>2</sub>C QDs, when pH is switched between 4 and 10. (C) Image of gel electrophoresis of mature miRNA-21 MB treated with DNase I for different times with or without Mo<sub>2</sub>C QDs protection. (D) Cell viabilities of B16-F10, MDA-MB-231, A549 and NHDF cells after incubation with Mo<sub>2</sub>C QDs at various concentrations for 24 h.

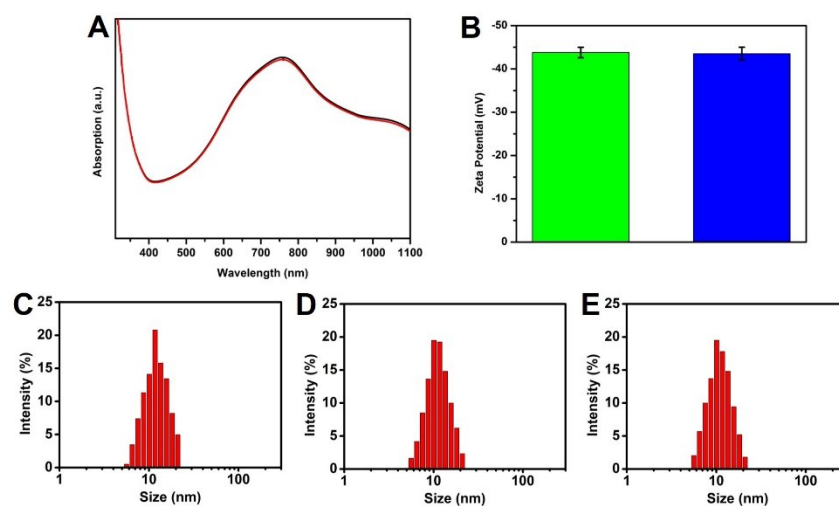


**Fig. S6.** (A) UV-vis-NIR spectra of Mo<sub>2</sub>C QDs (100 µg/mL, black line) and after two weeks of Mo<sub>2</sub>C QDs (100µg/mL, red line). (B) Zeta potentials of Mo<sub>2</sub>C QDs (100 µg/mL, green column) after two weeks of Mo<sub>2</sub>C QDs (100 µg/mL, blue column). Dynamic light scattering (DLS) of the Mo<sub>2</sub>C QDs in different media after two weeks: (C) deionized water; (D) high salt solution phosphate buffered saline and (E) cell medium.

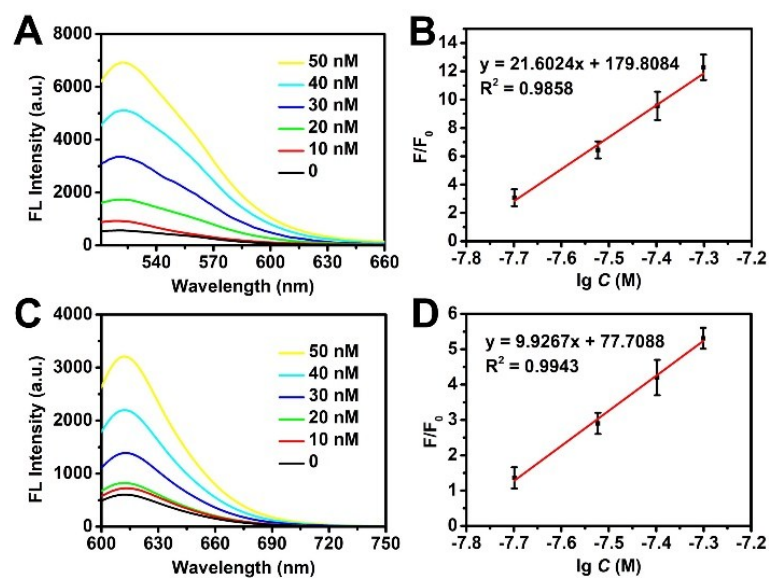


**Fig. S7.** Fluorescence emission spectra of Mo<sub>2</sub>C QDs nanoprobe (50 μg/mL loaded 50 nM mature miRNA-21 MB and 50 nM pre-miRNA-21 MB) incubated with different concentrations of (A) mature miRNA-21 and (C) pre-miRNA-21 at 37°C for 60 min. The corresponding calibration curve from different concentrations of target (B) mature miRNA-21 and (D) pre-miRNA-21.

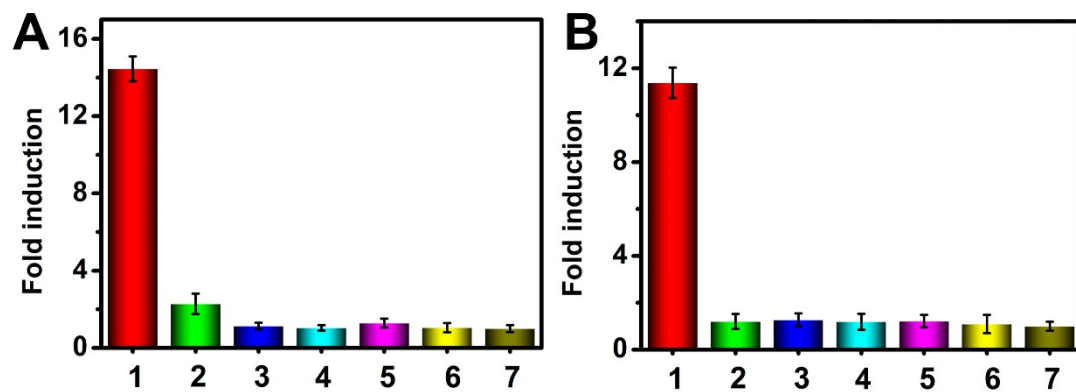


**Fig. S8.** Specificity evaluation for Mo<sub>2</sub>C QDs nanoprobe. (A) Specificity of the mature miRNA-21 MB for 50 nM different miRNA (1-7: miRNA-21, pre-miRNA-21, miRNA-373, miRNA-155, let-7a, NC and Blank); (B) Specificity of the pre-miRNA-21 MB for 50 nM different miRNA (1-7: pre-miRNA-21, miRNA-21, pre-miRNA-373, pre-miRNA-155, pre-let-7a, NC and Blank).

**Cellular uptake:** The cellular uptake procedure of the Mo<sub>2</sub>C QDs nanoprobe was also investigated. As shown in Fig. S8, the cellular uptake rate of Mo<sub>2</sub>C QDs nanoprobe in A549 cells was reduced to 46.5±6.4% at 4°C compared with the control group at 37°C. Low temperature can reduce the activity of enzymes in the cell, resulting in the reduction in mitochondrial energy production. The inhibition of cellular uptake at 4 °C suggested the cellular uptake procedure of the Mo<sub>2</sub>C QDs nanoprobe was mainly energy-dependent endocytosis and passive diffusion was also involved. Subsequently, different cell uptake inhibitors were applied to determine the endocytic pathways of Mo<sub>2</sub>C QDs nanoprobe. Colchicine and chlorpromazine were used to inhibit macro-pinocytosis and clathrin-mediated endocytosis pathways, respectively. The cellular uptake rate of Mo<sub>2</sub>C QDs nanoprobe in colchicine and chlorpromazine incubated A549 cells decreased by 22% and 27%, suggesting macro-pinocytosis and clathrin-mediated endocytosis were important ways to uptake Mo<sub>2</sub>C QDs nanoprobe.

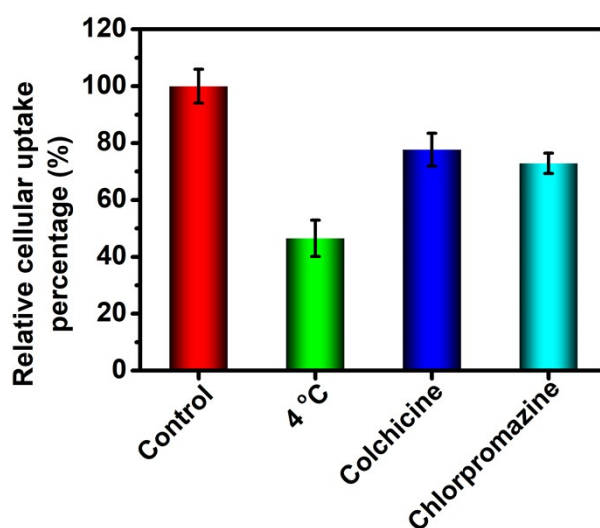


**Fig. S9.** ICP-MS analysis of cellular uptake pathways of Mo<sub>2</sub>C QDs nanoprobe.



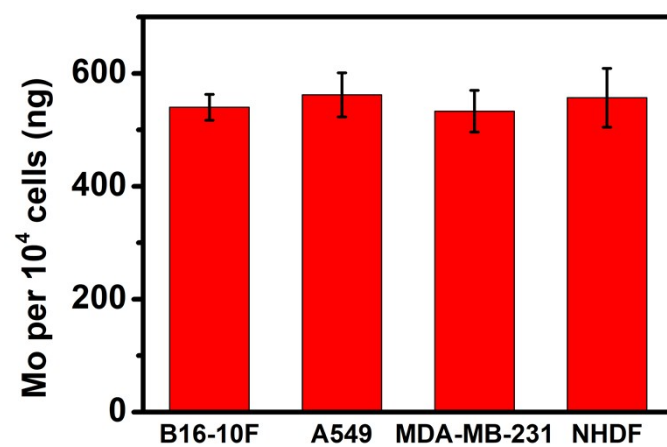


**Fig. S10.** Cellular internalization quantiles of the Mo<sub>2</sub>C QDs nanoprobe in different cell lines.

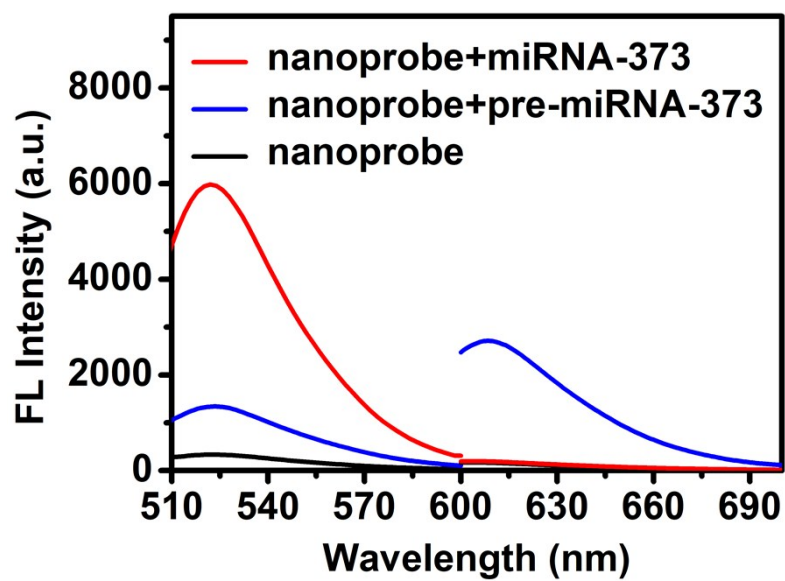


**Fig. S11.** The fluorescence emission spectra of mature miRNA-373 MB (50 nM) and pre-miRNA-373 MB (50 nM) mixed with miRNA-373 (50 nM) and pre-miRNA-373 (50 nM) at 37°C for 60 min.

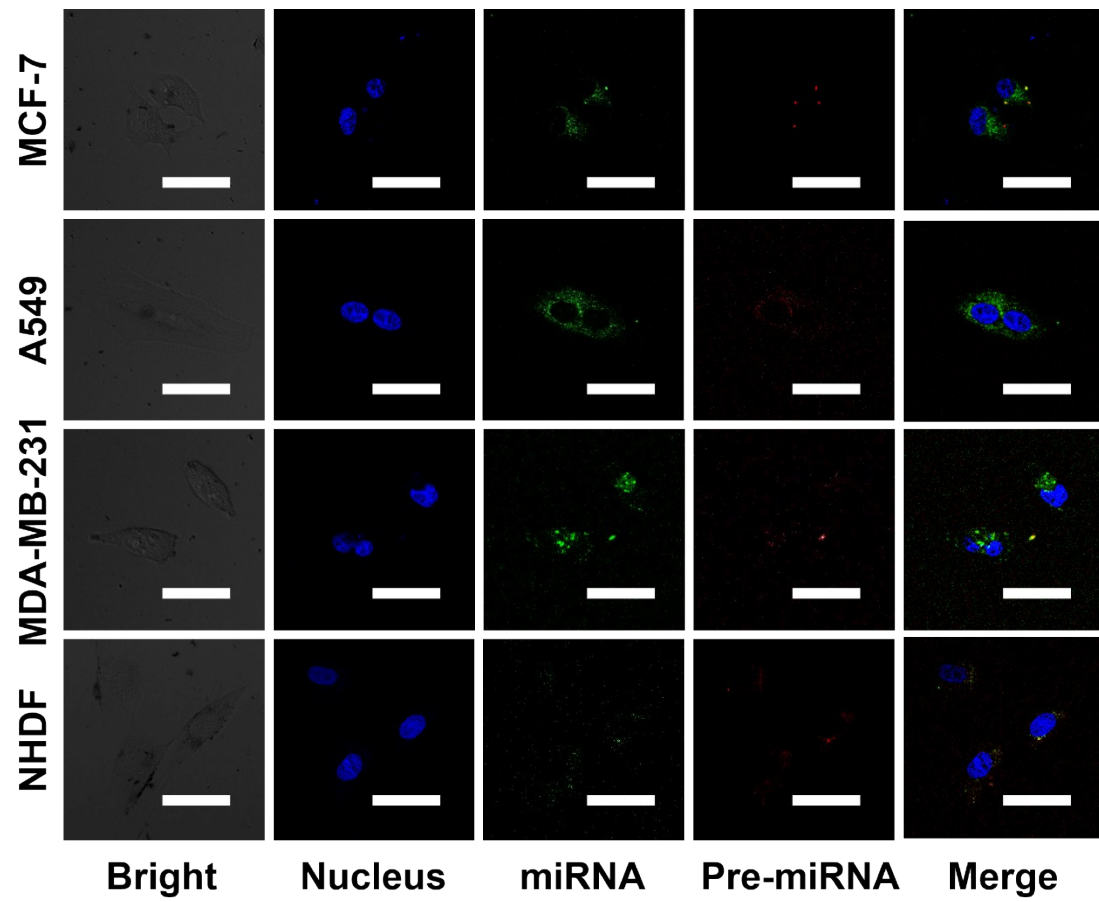


**Fig. S12.** Intracellular miRNA-373 accurate detection in different cell lines. miRNA-373 (green), pre-miRNA-373 (red) and nuclei (blue). Scale bar: 50  $\mu$ m.

**Table 1.** DNA and miRNA oligonucleotide sequences involved in this work.

Oligonucleotide	Sequence (5'---to---3')
miRNA-21 MB-1	FAM-AGA GTC AAC ATC AGT CTG ATA AGC TAC TCT-BHQ1
miRNA-21 MB-2	FAM-AGC GTC AAC ATC AGT CTG ATA AGC TAC GCT-BHQ1
miRNA-21 MB-3	FAM-AGC GTTC AAC ATC AGT CTG ATA AGC TAAC GCT-BHQ1
miRNA-21 MB-4	FAM-AGC GTTC AAC ATC AGT CTG ATA AGC TAC ACG CT-BHQ1
pre-miRNA-21 MB	ROX-CCT GTT GCC ATG AGA TTC AAC AGT CAA CAG G-BHQ2
miRNA-21	UAG CUU AUC AGA CUG AUG UUG A
pre-miRNA-21	UGU CGG GUA GCU UAU CAG ACU GAU GUU GAC UGU UGA AUC UCA UGG CAA CAC CAG UCG AUG GGC UGU CUG ACA
pre-miRNA-373	GGG AUA CUC AAA AUG GGG GCG CUU UCC UUU UUG UCU GUA CUG GGA AGU GCU UCG AUU UUG GGG UGU CCC
miRNA-373	GAA GUG CUU CGA UUU UGG GGU GU
miRNA-155	UUA AUG CUA AUC GUG AUA GGG GUU
let-7a	UGA GGU AGU AGG UUG UAU AGU U
NC	AUU GAA UAU UCU UAU UAU AAU UA
pre-miRNA-155	CUG UUA AUG CUA AUC GUG AUA GGG GUU UUU GCC UCC AAC UGA CUC CUA CAU AUU AGC AUU AAC AG
pre-let-7a	UGG GAU GAG GUA GUA GGU UGU AUA GUU UUA GGG UCA CAC CCA CCA CUG GGA GAU AAC UAU ACA AUC UAC UGU CUU UCC UA
miRNA-373 MB	FAM-AGC GAC ACC CCA AAA TCG AAG CAC TTC TCG CT-BHQ1
pre-miRNA-373 MB	ROX-CAT ATC CAG TAC AGA CAA AAA GGA TAT G-BHQ2

**References:**

- 1 W. Dai, H. Dong, B. Fugetsu, Y. Cao, H. Lu, X. Ma and X. Zhang, *Small*, 2015, **11**, 4158-4164.
- 2 M. Baker, G. Bao and C. Searles, *Nucleic Acids Res.*, 2012, **40**, e13.
- 3 A. James, M. Baker, G. Bao and C. Searles, *Theranostics*, 2017, **7**, 634-646.
- 4 W. Ma, P. Fu, M. Sun, L. Xu, H. Kuang and C. Xu, *J. Am. Chem. Soc.*, 2017, **139**, 11752-11759.
- 5 S. Li, L. Xu, M. Sun, X. Wu, L. Liu, H. Kuang and C. Xu, *Adv. Mater.*, 2017, **29**, 1606086.